Synthesis, spectroscopic and structural characterization of two (2,4,6-tribromophenyl)thiourea

N. Burcu Arslan (burcu.arslan@giresun.edu.tr)
Giresun University

Fatma Aydın
Çanakkale Onsekiz Mart University

Research Article

Keywords: (2,4,6-tribromophenyl)thiourea, Crystal structure, IR and NMR spectroscopy, electronic structure properties

Posted Date: November 23rd, 2023

DOI: https://doi.org/10.21203/rs.3.rs-3611555/v1

Additional Declarations: No competing interests reported.

Abstract

Two new compounds N-Benzoyl-N'-tribromophenyl thiourea ($C_{14}H_9Br_3N_2OS$) (I) and 4-Nitrobenzoyl-N'-tribromophenyl thiourea ($C_{14}H_8Br_3N_3O_3S$) (II) were synthesized and characterized by ^{1}HNMR, ^{13}CNMR, IR, and structural (XRD) techniques. The molecular geometry, vibrational frequencies of the title compound (I, II) in the ground state have been calculated by using the density functional theory (DFT) method with B3LYP / 6–311G(d,p) basis set and compared with the experimental data. The calculated results show that the optimized geometries can well reproduce the crystal structural parameters. A detailed vibrational spectral analysis has been carried out and assignments of observed fundamental bands have been proposed on the basis of peak positions. The scaled theoretical frequencies show very good agreement with experimental values. Frontier molecular orbitals energies (HOMO&LUMO), energy gap (ΔE), global chemical reactivity parameters such as ionization potential (IP), electron affinity (ΔE), chemical hardness (η) and chemical softness (σ), etc. have been calculated, the sites of electrophilic and nucleophilic regions where the molecular interactions likely to happen are identified. Besides, molecular electrostatic potential (MEP) and thermodynamic properties of the title compounds were investigated by theoretical calculations.

Introduction

The aroyl/acylthiourea derivatives due to the heteroatom content are known for their several biological activities, including antifungal, antibacterial, antiviral, anticancer insecticidal, herbicidal, etc. effects [1–5]. They are an important class of organic compounds having O-, N- and S- atoms. The amide, carbonyl, thioamide and thiocarbonyl groups with C(O)NHC(S)N core fragment that can participate to the tautomer are in the same molecule [6, 7] leading to physico-chemical and biological properties suitable for application in the field of coordination chemistry [8–10]. In addition, their derivatives consist of heteroatoms like nitrogen and sulfur which are nucleophilic centers, allowing the formation of inter- and intramolecular hydrogen bonds in the crystal structure [11–13].

Steric hindrance slows down chemical reactions due to steric mass [14]. Generally, steric hindrance gains importance in intermolecular reactions, but it also determines intermolecular interactions in the crystal lattice structure [15]. Also, it is often used to control selectivity, such as slowing down undesired side reactions [16, 17].

In present work, two novel compounds, N-Benzoyl-N2,4,6)- -tribromophenyl) thiourea (I) and N-(4-nitrobenzoyl)-N2,4,6)- -tribromophenyl) thiourea (II) were synthesized in high yield, via aroyl isocyanates and 2,4,6-tribromoaniline (Scheme 1). The structural characterization of the title compounds (I and II) have been confirmed using FT-IR, NMR, spectroscopy techniques and a single crystal X-ray diffraction method. The unit cells of crystals were compared with similar molecules in terms of steric hindrance. The geometrical parameters of the title compounds in the ground state have been calculated by using the density functional theory (DFT) methods with 6–311G(d,p) basis set and compared the experimental data. After on the optimization of molecular geometry, Molecular electrostatic potential (MEP) map, the

highest occupied molecular orbital (HOMO) and the lowest unoccupied molecular orbital (LUMO) analyses and thermodynamic properties were calculated by using density functional theory (DFT) with B3LYP/6-311G(d,p) level.

EXPERIMENTAL SECTION

Material and Measurements

All reagents (except 2,4,6-tribromoaniline) and solvents used in the synthesis were commercially purchased from Sigma-Aldrich, Merck Chemical. The melting points were determined in open capillary tubes by using an ElectroThermal IA 9100 apparatus. Reactions were monitored by thin-layer chromatography (TLC) on silica-gel 60 F254 plates (Merck). The infrared (FT-IR) spectrums were recorded on the Perkin Elmer Spectrum 100 FT-IR spectrometer in a spectral range of 4000 – 650 cm^{-1}. The ^{1}HNMR and ^{13}CNMR spectra were recorded on a JEOL ECX-400 FT-NMR spectrometer operating at 400 and 100 MHz, respectively, using DMSO- d_6 as solvent. The crystal structure analysis of the title compounds were carried out using a Bruker APEX-II CCD X-ray diffractometer (MoK_{α} radiation, 0.71073 Å).

Synthesis and Characterization

The synthesis of N-Benzoyl-N2,4,6)-□-tribromophenyl)-thiourea (I) and N-4-Nitro-benzoyl-N2,4,6)-□-tribromophenyl)-thiourea (II)

2,4,6-tribromoaniline was synthesized as literature [15]. A solution of aroyl chloride (benzoyl- and 4-nitrobenzoyl-; 2.32 mL and 3.70 g, 20 mmol) in dry acetone (20 mL) were added drop wise to a three-necked round-bottomed flask containing potassium thiocyanate solution in acetone (10 mL) (1.94 g, 20 mmol). The mixtures were refluxed for approximately 1 hour and then cooled to room temperature. Then a solution of 2,4,6-tribromoaniline (0.652 g, 20 mmol) in dry acetone (20 ml) was added dropwise over 0.5 h, without filtration obtained white color benzoyl isothiocyanate and pale yellow color 4-nitrobenzoyl isothiocyanate and the mixture was stirred for 2 and 3 h., respectively. The resulting mixture was pushed into 100 mL water and filtered off, washed with hot water to remove inorganic salts and dried in vacuum. After then, raw product was chromatographed over silica gel using ethyl acetate-hexane (4:1) as the eluent to separate the product. After evaporation the solvent, the fairly pure, colourless (I) and pale yellow color (II) products were crystallized out, respectively, (Scheme 1)

Compound I: Colourless crystals, Yield: 0.850 g, 87% and m.p.: 207–208 °C, FT-IR (cm^{-1}): 3255 (N-H), 3099, 3074, 3003 ($C_{aromatic}$ -H), 1670 (C = O), 1506 (N-CS, thioureido), 1151 (N-CO), 1343 (C = Caromatic), 778(C = S, stretching), 682 (C-Br); ^{1}H-NMR (400 MHz, DMSO-d_6, ppm) 12,08 (s, 1H, NH), 11.94 (s, 1H, NH), 8.03 (s, 2H, $Ar(Br)_3$-H), 8.01 (d, J = 7.7 Hz, 2H, ph-H) 7.68 (t, 2H, ph-H), 7.56(s, 2H, ph-H); ^{13}C NMR (100

MHz, DMSO-d_6, δ ppm): 180.75 (C = S), 168.04 (C = O), 136.94, 131.71, 128.50, 121.40 ($Ar(Br)_3$-C), 134.23,133.34, 128.76, 125.08 (ph-C).

Compound II: Pale yellow crystals, Yield: g, 72%, FT-IR (cm^{-1}): 3413 (N-H), 3284 (N-H), 3150, 3095, 3073 ($C_{aromatic}$ -H), 1728 (C = O), 1607 (C = C), 1454 (-C = N), 1539 (C = S), 1381 (C = $C_{aromatic}$), 858 (ON = O), 742(C = S), 729, 682 (C-Br); ^{1}H-NMR (400 MHz, DMSO- d_6, ppm) 12.25 (s, 1H, NH), 11.86 (s, 1H, NH), 8.31 (d, 2H, $Ar(NO_2)$-H), 8.17 (d, J = 7.7 Hz, 2H, $Ar(NO_2)$-H) 7.99 (s, 2H, $Ar(Br)_3$-H); ^{13}C NMR (100 MHz, DMSO-d_6, δ ppm): 180.91 (C = S), 167.09 (C = O), 138.04, 134.78, 125.56, 122.04 ($Ar(Br)_3$-C), 150.46, 137.42, 130.91, 123.95 (Ar(NO2)-C.

Xray Data Collection and Structure Refinement

The single crystal X-ray data were collected on a Bruker APEX-II. All diffraction measurements were performed at room temperature (296 K) using graphite monochromated Mo K*α* radiation (λ = 0.71073 Å). Unit cell parameters were determined from least-squares refinement of setting angels with θ for the compounds in the range $2.9 \leq \theta \leq 26$ and $2.9 \leq \theta \leq 25.1$, respectively. The structures were solved by direct methods using SHELXS-97 [18] implemented in the WinGX [19] program suite. The refinement were carried out by full-matrix least-squares method on the positional and anisotropic temperature parameters of the non-hydrogen atoms, or equivalently corresponding to 380 crystallographic parameters for compound I and 181 crystallographic parameters for compound II, using SHELXL-97 [18]. All of the H atoms of the compound I and compound II were positioned geometrically and treated using a riding model, fixing the bond lengths at 0.86 and 0.93 Å for NH and CH atoms, respectively. Details of the data collection conditions and the parameters of refinement processes for the two compounds are given in Table 1. The atomic numbering schemes with displacement ellipsoids of the crystal structures drawing with ORTEP III [19]were depicted at the 30% probability level for clarity (Fig. 1 and Fig. 2).

Table 1
Crystal data and structure refinement parameters for the title compounds (I) and (II).

Parameters	Compound I	Compound II
Empirical Formula	$C_{14}H_9Br_3N_2OS$	$C_{14}H_8Br_3N_3O_3S$
Formula Weight	493.02	538.02
Crystal System / Space Group	Monoclinic / P 2_1/n	Orthorhombic / P b c a
a / Å	8.0437(13)	16.5477(12)
b / Å	37.021(6)	7.4257(6)
c / Å	10.7842(15)	28.378(2)
α / °	90	90
β / °	90.936(5)	90
γ / °	90	90
V / Å^3	3210.9(8)	3487.1(5)
Z	8	8
D_{calc} (Mg/m^3)	2.040	2.050
μ (mm^{-1})	7.666	7.077
Crystal size (mm)	0.12×0.09×0.07	0.09×0.07×0.03
Colour / Shape	Colourless / Prism	Pale yellow / Block
Temp (K)	293	293
Theta range for collection	2.9 ≤ θ ≤ 26	2.9 ≤ θ ≤ 25.1
Reflections collected	36579	27641
Independent reflections	6301	3061
Data/restraints/parameters	6301/0/380	3061/0/181

Computational Procedures

The ground state geometry of title compounds I and II which are taken from the crystal structure were optimized using standard density functional theory (DFT) [20] level of B3LYP [21] with a 6-311G(d,p) [22] basis set using Gaussian 09 program [23]. After optimization, the quantum chemical calculations were calculated and MEP [24] surface map was obtained. Thus from the results of the MEP map, the chemical reactivity of the compound could be easily estimated. Additionally, HOMO-LUMO gaps and FT-IR

spectrum were calculated at the same basis set. Calculated vibrational frequencies of the optimized molecular structure then scaled by 0.962 [25] for DFT. Vibrational band assignments were made using the Gauss-View molecular visualization program [26].

Results and discussion

Description of Crystal Structure

As shown in Fig. 1 and Fig. 2, the crystals of compound (I) and compound (II) crystallizes in the monoclinic space group P 21/n and orthorhombic space group P b c a, respectively, with Z = 8. Both molecules have thiourea, 2,4,6-tribromophenyl and phenyl groups in common. The torsion angles between the 2,4,6-tribromophenyl and thiourea groups at the title compounds are 96.2° and 84.0°, respectively. In compound (I) molecular packing contains three different types of hydrogen bond between C—H…Br, N—H…O and N—H…S atoms which are tabulated in Table S1. The N atom of thiourea group acts as a donor atom to benzoyl oxygen atom with the donor acceptor distance 3.273 Å and symmetry code (x,+y,+z-1). The other N atom of the same thiourea group also acts as a donor to thiourea group S atom with the donor acceptor distance 3.353 Å and symmetry code (x,+y, + z + 1). The combination of these hydrogen bonds generates a $R_2^2\ (10)$ ring running parallel to [001] Figure S1.

Similarly to compound (I), compound (II) has a N—H…S type hydrogen bonding with the donor acceptor distance 3.616 Å and symmetry code (-x + 1,-y + 2,-z + 1). This bonding generates the $R_1^1\ (8)$ ring running parallel to [100]. Also there is an intramolecular hydrogen bond between thiourea N atom and benzoyl O atom as seen at Table S2 and Figure S2.

Spectral Analysis

Vibrational Spectra

The IR spectra of the compound showed absorption of the carbonyl group at 1659 and 1607 cm^{-1} (υ C = O), thiocarbonyl group at 861 and 858 cm^{-1} (υ C = S) and amide group at 3255 and 3413 cm^{-1} (υ N-H), respectively. Vibration bands with the wave numbers of 3099, 3074 and 3284, 3073 cm^{-1} (υ C-H, Ar-H); 1670 and 1728 cm^{-1} (υ C = O); 1603 and 1539 cm^{-1} (υ C = C); 1506 and 1454 cm^{-1} (υ -CO-N), 1343 cm^{-1} and 1381 cm^{-1} (CS-N) were observed for compound respectively. Besides, the -N-CS- group was observed as a band at 1151 cm^{-1}. The stretching of the C-Br bonds for compounds were confirmed at 779, 739 and 684 and 842, 729 and 705 cm^{-1}, respectively. (Fig. 3 and Fig. 4)

NMR Analysis

In the ^{1}H NMR, the characteristic broad singlet peaks appeared at δ 12.08, 12.25 ppm and 11.94 ppm, 11.86 ppm, for amide protons (NH) and thio-amide protons (NH') were confirmed the structure of the new title compounds I and II, respectively. For the title compounds I and II, the proton peaks of phenyl ring 7.56

ppm (m, 1H), 7.68 (t, 2H), 8.01 ppm (d, 2H) and 4-nitrophenyl ring 8.17 ppm (d, 2H), 8.31 ppm (d, 2H) could be observed. Also, the peaks of tribromo-phenyl rings of the compound I and II were observed at 8.03 ppm (s, 2H) and 7.99 ppm (s, 2H), respectively. In the ^{13}C NMR spectra of the title compounds I and II, the signals observed in the region of the δ 168.0 and 167.0 ppm and δ 180.7 and δ 180.9 ppm describe the C = O and C = S carbons, respectively. Additionally, the peaks observed in the aromatic region confirmed the structures (Scheme 2).

Mulliken Atomic Charges Analysis

Since atomic charges determine the dipole moment, molecular polarization and bond properties of a molecule The Mulliken atomic charge calculation plays an important role [27]. Mulliken population analysis was performed using the DFT/B3LYP calculation method with 6-311 + G(d,p) basis set for the title compounds. Graphical reorientations of Mulliken charge distributions of the title compounds I and II is shown in Fig. 5. The hydrogen atoms are all positively charged, but those bonded to the nitrogen atoms are the most positively charged. Similarly, the nitrogen atoms conjugated with the carbonyl and thiocarbonyl group of the title compounds I and II are highly negatively charges, (-0.392 -0.414 esu and −0.407, -0.418 esu), respectively, while the nitrogen atom of the nitro group of the compound II has a positive charge (0.186 esu). In compound I and II, it has been observed that the carbon atoms in the phenyl ring to which it is attached have a negative charge, while the bromine atoms have very little positive charge (0.004–0.017, 0.009–0.027 asu), respectively. The highest positive atomic charge was 0.466 in compound I, also with 0.492 compound II has higher positive carbon atom charge of the carbonyl group. Therefore, the carbonyl groups are reactive moiety in these compounds.

Molecular Electrostatic Potential (MEP)

Molecular electrostatic potential (MEP) helps to interpret detailed information about many properties of a compound such as chemical reactivity or the biological activity. The spatial distribution and values of the electrostatic potential determine the attack regions of an electrophilic or a nucleophilic unit to the molecule [28]. The total electronic density and the MEP surface of the title molecules are constructed by the B3LYP/6-311G (d,p) method and are shown in Fig. 6. The electronegative and electropositive regions of the MEP surface are identified by the color scheme. Red color is rich in electrons and partially negatively charged; yellow and green are defined as the neutral ranges and blue as the electron-deficient, partially positive charge region [29]. These MEP maps for the title compounds I and II show that the sulfur atom, as well as the carbonyl oxygen atom, is a possible site for electrophilic attack due to the tribromophenyl ring, and the nucleophilic attack sites are located on the hydrogen atoms bonded to nitrogen atoms. These MEP maps for compounds I and II show that the S atom, as well as the carbonyl O atom, is a possible site for electrophilic attack due to the tribromophenyl ring, and the nucleophilic attack sites are located on the hydrogen atoms bonded to nitrogen atoms. The results show that the most reactive region of these compounds is the region containing the sulfur atom, and also provide information about the region where the compound may have intermolecular hydrogen bond interactions.

Frontier Molecular Orbitals Analysis

Frontier molecular orbitals (FOM's), as known the highest occupied molecular orbital (HOMO) and lowest unoccupied molecular orbital (LUMO), contain information about the chemical stability of the molecule [30]. The active regions can be predicted by the distribution of frontier orbital since the HOMO implies the electron-donating ability of a molecule and the LUMO indicates the electrons-accepting capacity of a molecule [31]. The HOMO-LUMO plots of the two molecules are shown in Fig. 7. The negative and positive phases are represented in red and green color. As shown at the Fig. 7, the HOMO electrons are localized around entire tribromophenyl and connected thiourea moiety while LUMO the electrons are distributed entirely over the aroyl ring and thiourea moiety for the title compounds.

According to B3LYP/6-311G(d,p) method, the HOMO-LUMO and energy gap values of the title compound molecules were calculated as energies 6.1072 eV (HOMO), 6.2569 eV (HOMO-1), -2.2939 eV (LUMO), -2.0563 eV (LUMO-1) and 6.6841 eV (HOMO), 6.9641 eV (HOMO-1), -3.1891 eV (LUMO), -1.9157 eV (LUMO + 1), 3.4950 eV, respectively. Comparing the energy gap values of the title compounds, compound II is more chemical reactive and unstable than compound I because the energy gap is narrower due to the effect of the nitro group. In addition to this, the global reactivity of the title compounds such as chemical potential (μ), chemical hardness (η), global electrophilicity index (ω), and chemical softness (ς) were calculated and listed in Table 2.

Table 2
Frontier orbital energies, HOMO-LUMO energy gap, ionization potential (I), Electron affinity (A), chemical potential (μ), chemical hardness (η), absolute softness (ζ), absolute electronegativity (χ), chemical potential (μ), and electrophilicity index (ω) of title compounds for ground state geometries in gas phase at B3LYP/6-311G(d,p) level.

Parameters B3LYP/6-311G(d,p)	Compound (I) (eV)	Compound (II) (eV)
Electronic Energy (a.u.)	-17688.9911	-9049.0604
E_{HOMO}	6.1072	6.6841
E_{LUMO}	-2.2939	-3.1891
Ionization energy, $I = -E_{HOMO}$	-6.1072	-6.6841
Electron affinity, $A = -E_{LUMO}$	2.2939	3.1891
Energy band gap, [$\Delta E = E_{HOMO}-E_{LUMO}$]	8.4011	9.8732
Chemical hardness, η = (I-A) / 2	-4.2005	-4.9366
Chemical softness, ζ = 1/2η	-0,1190	-0,1013
Electronegativity, χ = (I + A) / 2	4,2006	-1,7475
Chemical potential, μ = - (I + A) / 2	1,9067	1,7475
Electrophilicity index, ω = μ²/2 η	-0,4327	-0,3092

Thermodynamic Properties

Thermodynamic quantum chemical data becomes important to study the reaction processes of organic compounds [32]. Thermodynamic parameters for different temperatures were calculated at the B3LYP/6-311G (d,p) level and scaled by 0.96. Three main thermodynamic properties as heat capacity ($C°_{p,m}$), enthalpy ($H°_m$) and entropy ($S°_m$) for the title compounds I and II are plotted at Fig. 8a,b and listed Table S3,4. As shown in Fig. 8, all the values rise when the temperature increases in the range of 100–1000 K.

The correlation equation of $C^0_{p,m}$, S^0_m, H^0_m and temperature are as follows for title compounds I and II, respectively:

$C^{\circ}_{p.m}$ = 13.7884 + 0.2660 T -1.279 x10^{-4} T^2 (R^2 = 0.9991)

S°_{m} = 79.7534 + 0.3501 T – 1.0782x10^{-4} T^2 (R^2 = 0.9996)

ΔH^0_m = -4.2287 + 0.0491 T + 6.1967x10^{-5} T^2 (R^2 = 0.9993)

$C^{\circ}_{p,m}$ = 26.5639 + 0.4899 T -2.3069x10^{-4} T^2 (R^2 = 0.9992)

S_m° = 112.2255 + 0.6415 T – 1.93958x10^{-4} T^2 (R^2 = 0.9996)

ΔH_m^0 = -7.5617 + 0.0884 T + 7.4451x10^{-6} T^2 (R^2 = 0.9993)

Additionally, for both title compounds, all calculated thermodynamic parameters ($C^0_{p,m}$, S^0_m, H^0_m) appear to increase with increasing temperature due to the increase in molecular vibration.

Conclusion

In this study, two novel, $C_{14}H_9N_3OSBr_3$, N-(benzoyl)-N-(2,4,6-tribromophenyl)-thiourea and $C_{14}H_8N_3O_3SBr_3$, N-(4-nitrophenyl)-N-(2,4,6-tribromophenyl)-thiourea have been synthesized and investigated by elemental analysis, FT – IR and structural X-ray diffraction techniques. ^{1}H-NMR, ^{13}C-NMR spectroscopy analyses have also been done for the compounds.

The theoretical calculations of these compounds have also been performed by using the density functional theory (DFT) method with the B3LYP / 6–311G(d,p) basis set. Although the differences observed in the geometric parameters, the general agreement are in a good range and the theoretical calculations support the solid state structures. The experimental vibrational frequencies are in agreement with the results of B3LYP method. The calculated MEP maps verify the intramolecular hydrogen bond interactions in solid states. HOMO and LUMO's are come into existence with π-antibonding type orbitals.

Declarations

Conflict of interest The authors declare that they have no competing financial interests or personal relationships that could affect the study reported in this article.

Data Availability

CCDC 2160417 and 2160418 contains the supplementary crystallographic data (excluding structure factors) for the structures I and II, respectively, reported in this article. These data can be obtained free of charge via http://www.ccdc.cam.ac.uk/data_request/cif, by e-mailing at data_request@ccdc.cam.ac.uk or by contacting The Cambridge Crystallographic Data Centre, 12, Union Road, Cambridge CB2 1EZ, UK; fax: +44-1223-336033. The authors declare that all other data supporting the findings of this study are available within the article and its supplementary information files.

References

1. B. Özgeriş, "Design, synthesis, characterization, and biological evaluation of nicotinoyl thioureas as antimicrobial and antioxidant agents.," *J. Antibiot. (Tokyo).*, vol. 74, no. 4, pp. 233–243, Apr. 2021, doi: 10.1038/s41429-020-00399-7.
2. A. Rana, N. Siddiqui, S. A. Khan, S. Ehtaishamul Haque, and M. A. Bhat, "N-{[(6-Substituted-1,3-benzothiazole-2-yl)amino]carbonothioyl}-2/4-substituted benzamides: Synthesis and

pharmacological evaluation," *Eur. J. Med. Chem.*, vol. 43, no. 5, pp. 1114–1122, May 2008, doi: 10.1016/j.ejmech.2007.07.008.

3. F. Asghar, S. Rana, S. Fatima, A. Badshah, B. Lal, and I. S. Butler, "Biologically active halo -substituted ferrocenyl thioureas: synthesis, spectroscopic characterization, and DFT calculations," *New J. Chem.*, vol. 42, no. 9, pp. 7154–7165, 2018, doi: 10.1039/C8NJ00483H.
4. L. K. Soni, T. Narsinghani, and R. Jain, "Synthesis and Antibacterial Screening of Some 1-Aroyl-3-aryl Thiourea Derivatives," *ISRN Med. Chem.*, vol. 2014, p. 393102, 2014, doi: 10.1155/2014/393102.
5. L.-P. Duan, J. Xue, L.-L. Xu, and H.-B. Zhang, "Synthesis 1-Acyl-3-(2'-aminophenyl) thioureas as Anti-Intestinal Nematode Prodrugs," *Molecules*, vol. 15, no. 10, pp. 6941–6947, 2010, doi: 10.3390/molecules15106941.
6. M. Shaabanzadeh and F. Khabari, "One-pot diastereoselective synthesis of new spiro indenoquinoxaline derivatives containing cyclopropane ring," *Arkivoc*, vol. 2009, no. 11, pp. 307–315, Sep. 2009, doi: 10.3998/ark.5550190.0010.b28.
7. F. Aydın, H. Ünver, D. Aykaç, and N. O. İskeleli, "Spectroscopic Studies and Structure of 4-(3-Benzoylthioureido)benzoic Acid," *J. Chem. Crystallogr.*, vol. 40, no. 12, pp. 1082–1086, Dec. 2010, doi: 10.1007/s10870-010-9799-2.
8. C. K. Ozer, G. Binzet, and H. Arslan, "Crystal and molecular structure of bis(N-(diethylcarbamothioyl)cyclohexane carboxamido)copper(II) complex," *Eur. J. Chem.*, vol. 11, no. 4, pp. 319–323, Dec. 2020, doi: 10.5155/eurjchem.11.4.319-323.2047.
9. U. Solmaz *et al.*, "Synthesis, characterization, crystal structure, and antimicrobial studies of novel thiourea derivative ligands and their platinum complexes," *J. Coord. Chem.*, vol. 71, no. 2, pp. 200–218, Jan. 2018, doi: 10.1080/00958972.2018.1427233.
10. R. C. Luckay, F. Mebrahtu, C. Esterhuysen, and K. R. Koch, "Extraction and transport of gold(III) using some acyl(aroyl)thiourea ligands and a crystal structure of one of the complexes," *Inorg. Chem. Commun.*, vol. 13, no. 4, pp. 468–470, Apr. 2010, doi: 10.1016/j.inoche.2010.01.010.
11. F. Aydin, D. Aykaç, N. Burcu Arslan, and C. Kazak, "STRUCTURE OF ORGANIC COMPOUNDS Synthesis, Characterization, and Crystal Structure of Bis[4-(3'-benzoyl)thiocarbamidophenyl]ether 1," *Crystallogr. Reports*, vol. 59, no. 7, pp. 955–960, 2014, doi: 10.1134/S1063774514070050.
12. E. Contreras Aguilar *et al.*, "Acyl thiourea derivatives: A study of crystallographic, bonding, biological and spectral properties," *Chem. Phys. Lett.*, vol. 715, pp. 64–71, Jan. 2019, doi: 10.1016/j.cplett.2018.11.020.
13. F. Aydin and N. B. Arslan, "Synthesis, Crystal Structure and Cyclic Voltammetric Behavior of N-aroyl-N'-(4'-cyanophenyl)-thioureas," *Molbank*, vol. 2022, no. 1, p. M1316, Jan. 2022, doi: 10.3390/M1316.
14. B. Pinter, T. Fievez, F. M. Bickelhaupt, P. Geerlings, and F. De Proft, "On the origin of the steric effect," *Phys. Chem. Chem. Phys.*, vol. 14, no. 28, p. 9846, 2012, doi: 10.1039/c2cp41090g.
15. T. Geiger, A. Haupt, C. Maichle-Mössmer, C. Schrenk, A. Schnepf, and H. F. Bettinger, "Synthesis and Photodimerization of 2- and 2,3-Disubstituted Anthracenes: Influence of Steric Interactions and

London Dispersion on Diastereoselectivity," *J. Org. Chem.*, vol. 84, no. 16, pp. 10120–10135, Aug. 2019, doi: 10.1021/acs.joc.9b01317.

16. O. Y. Audu, J. Jooste, F. P. Malan, O. O. Ajani, and N. October, "Synthesis, characterization, molecular structure, and computational studies on 4(1H)-pyran-4-one and its derivatives," *J. Mol. Struct.*, vol. 1245, p. 131077, Dec. 2021, doi: 10.1016/j.molstruc.2021.131077.
17. I. A. Udofia *et al.*, "Experimental and theoretical calculation of pKa values of substituted-2,4,6-trinitrodiphenylamines," *J. Mol. Liq.*, vol. 371, p. 120926, Feb. 2023, doi: 10.1016/j.molliq.2022.120926.
18. G.M. Sheldrick, "SHELXS-97 and SHELXL-97 Program for Crystal Structure Solution and Refinment University of Gottingen, Germany," *Univ. Gottingen, Ger.*, 1997.
19. L. J. Farrugia, "WinGX and ORTEP for Windows: an update," *J. Appl. Crystallogr.*, vol. 45, no. 4, pp. 849–854, Aug. 2012, doi: 10.1107/S0021889812029111.
20. A. D. Becke, "Density-functional thermochemistry. III. The role of exact exchange," *J. Chem. Phys.*, vol. 98, no. 7, pp. 5648–5652, 1993, doi: 10.1063/1.464913.
21. C. Lee, W. Yang, and R. G. Parr, "Development of the Colle-Salvetti correlation-energy formula into a functional of the electron density," *Phys. Rev. B*, vol. 37, no. 2, pp. 785–789, Jan. 1988, doi: 10.1103/PhysRevB.37.785.
22. R. Ditchfield, W. J. Hehre, and J. A. Pople, "Self-Consistent Molecular-Orbital Methods. IX. An Extended Gaussian-Type Basis for Molecular-Orbital Studies of Organic Molecules," *J. Chem. Phys.*, vol. 54, no. 2, pp. 724–728, Jan. 1971, doi: 10.1063/1.1674902.
23. D. J. Frisch, M. J.; Trucks, G. W.; Schlegel, H. B.; Scuseria, G. E.; Robb, M. A.; Cheeseman, J. R.; Scalmani, G.; Barone, V.; Mennucci, B.; Petersson, G. A.; Nakatsuji, H.; Caricato, M.; Li, X.; Hratchian, H. P.; Izmaylov, A. F.; Bloino, J.; Zheng, G.; Sonnenb, "Gaussian, Inc." Wallingford CT, 2009. [Online]. Available: https://gaussian.com/g09citation/
24. K. Sen J.S. Murray, "Molecular Electrostatic Potentials, Volume 3 1st Edition Concepts and Applications, Elsevier Science," 1996.
25. M. P. Andersson and P. Uvdal, "New Scale Factors for Harmonic Vibrational Frequencies Using the B3LYP Density Functional Method with the Triple-ζ Basis Set 6-311+G(d,p)," *J. Phys. Chem. A*, vol. 109, no. 12, pp. 2937–2941, Mar. 2005, doi: 10.1021/jp045733a.
26. T. K. Roy Dennington and J. Millam, "Gaussview Version 5, 2009," *Semichem Inc. Shawnee Mission KS*.
27. R. S. Mulliken, "Electronic Population Analysis on LCAO–MO Molecular Wave Functions. I," *J. Chem. Phys.*, vol. 23, no. 10, pp. 1833–1840, Dec. 2004, doi: 10.1063/1.1740588.
28. E. . T. J. Scroccoand, *E.ScroccoandJ.Tomasi,Electronicmolecularstructure, reactivity and intermolecular forces: Anheuristic interpretation by means of electrostaticmolecular potentials*, Ed. P.O. NewYork: Lowdin, AcademicPress, 1978.
29. P. Geerlings, F. De Proft, and P. W. Ayers, "Chapter 1 Chemical reactivity and the shape function," in *Theoretical Aspects of Chemical Reactivity*, vol. 19, A. B. T.-T. and C. C. Toro-Labbé, Ed. Elsevier, 2007,

pp. 1–17. doi: https://doi.org/10.1016/S1380-7323(07)80002-1.

30. R. G. Pearson, “Chemical hardness and density functional theory,” *J. Chem. Sci.*, vol. 117, no. 5, pp. 369–377, 2005, doi: 10.1007/BF02708340.
31. Y. Xu, Q. Chu, D. Chen, and A. Fuentes, “HOMO–LUMO Gaps and Molecular Structures of Polycyclic Aromatic Hydrocarbons in Soot Formation,” *Front. Mech. Eng.*, vol. 7, 2021, doi: 10.3389/fmech.2021.744001.
32. L. Jean-Pierre, “The Role and the Status of Thermodynamics in Quantum Chemistry Calculations,” J. C. Moreno-Pirajan, Ed. Rijeka: IntechOpen, 2011, p. Ch. 18. doi: 10.5772/23465.

Schemes

Schemes 1 and 2 are available in the Supplementary Files section.

Figures

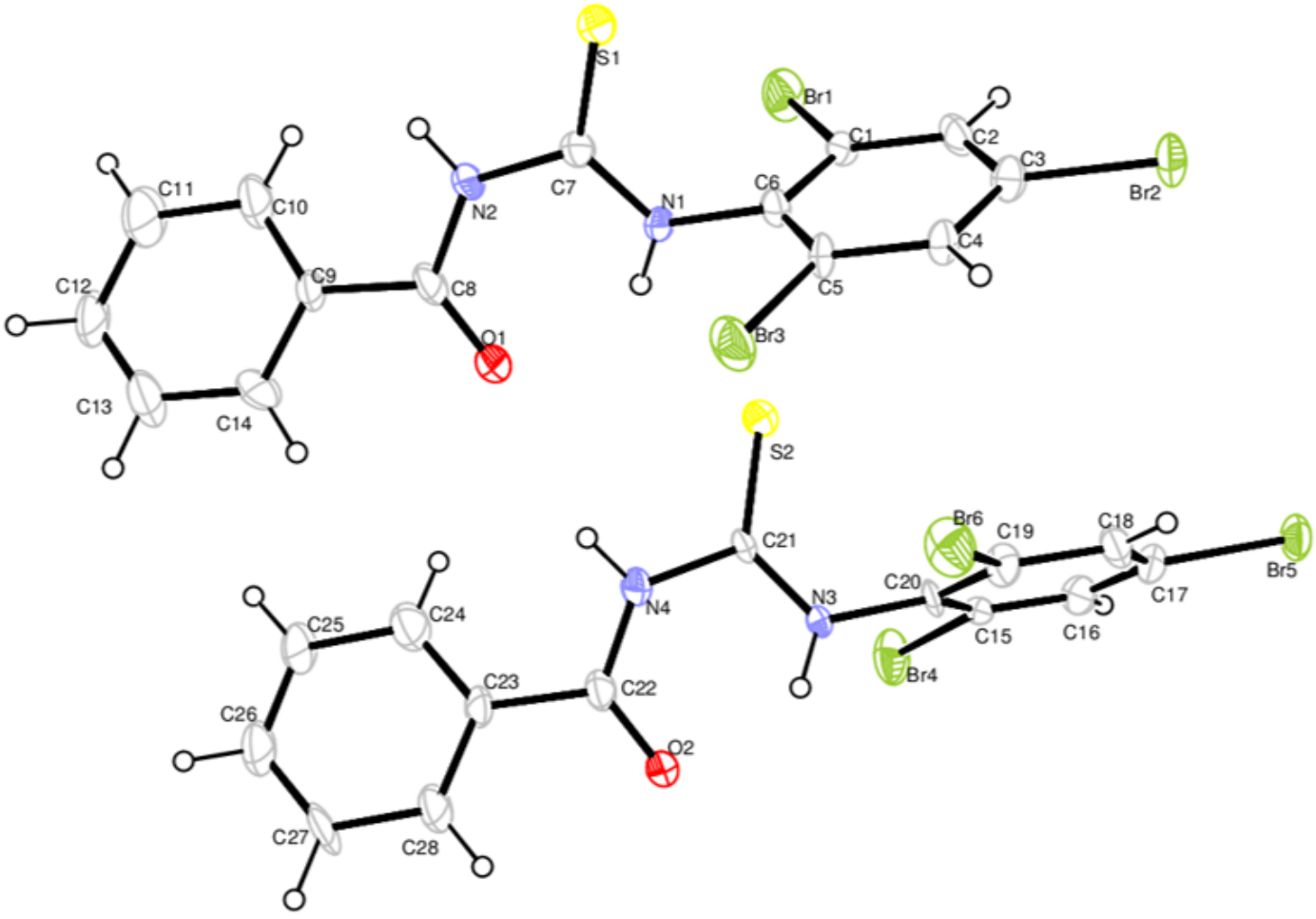

Figure 1

A view of the title compound I showing the atom-numbering scheme. Displacement ellipsoids are drawn at the 30% probability level and H atoms are shown as small spheres of arbitrary radii.

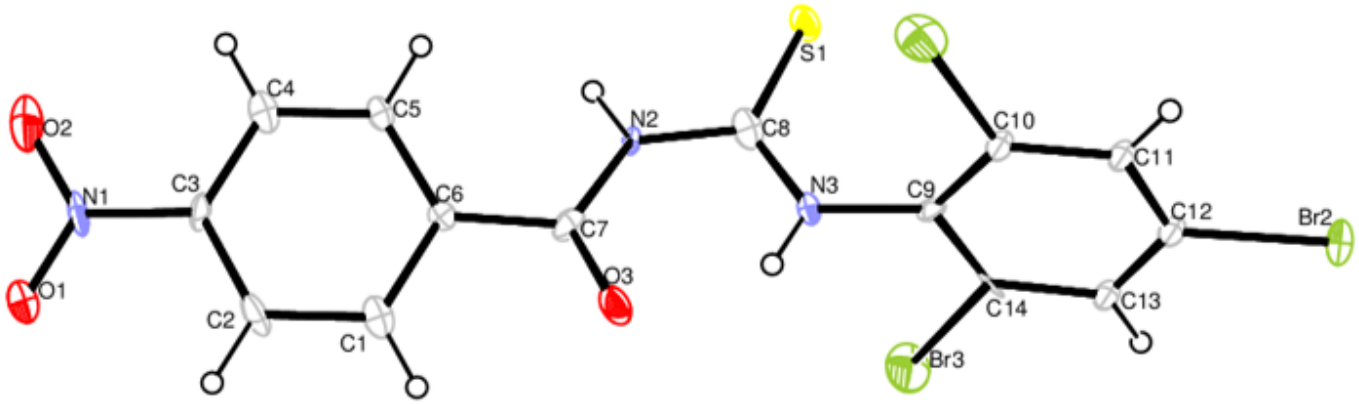

Figure 2

A view of the title compound II showing the atom-numbering scheme. Displacement ellipsoids are drawn at the 30% probability level and H atoms are shown as small spheres of arbitrary radii.

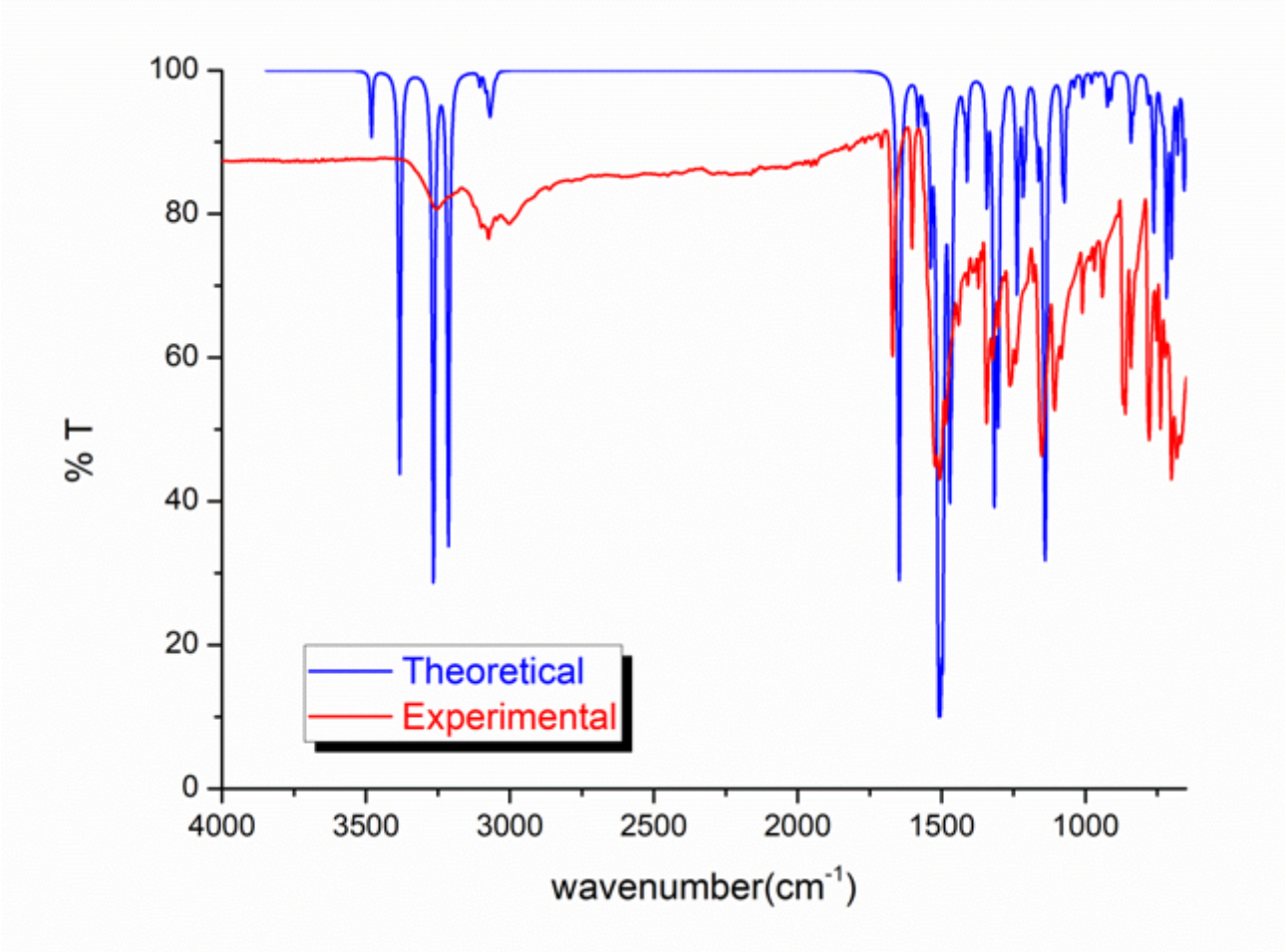

Figure 3

Experimental FT-IR and simulated FT-IR spectra of the title compound (I).

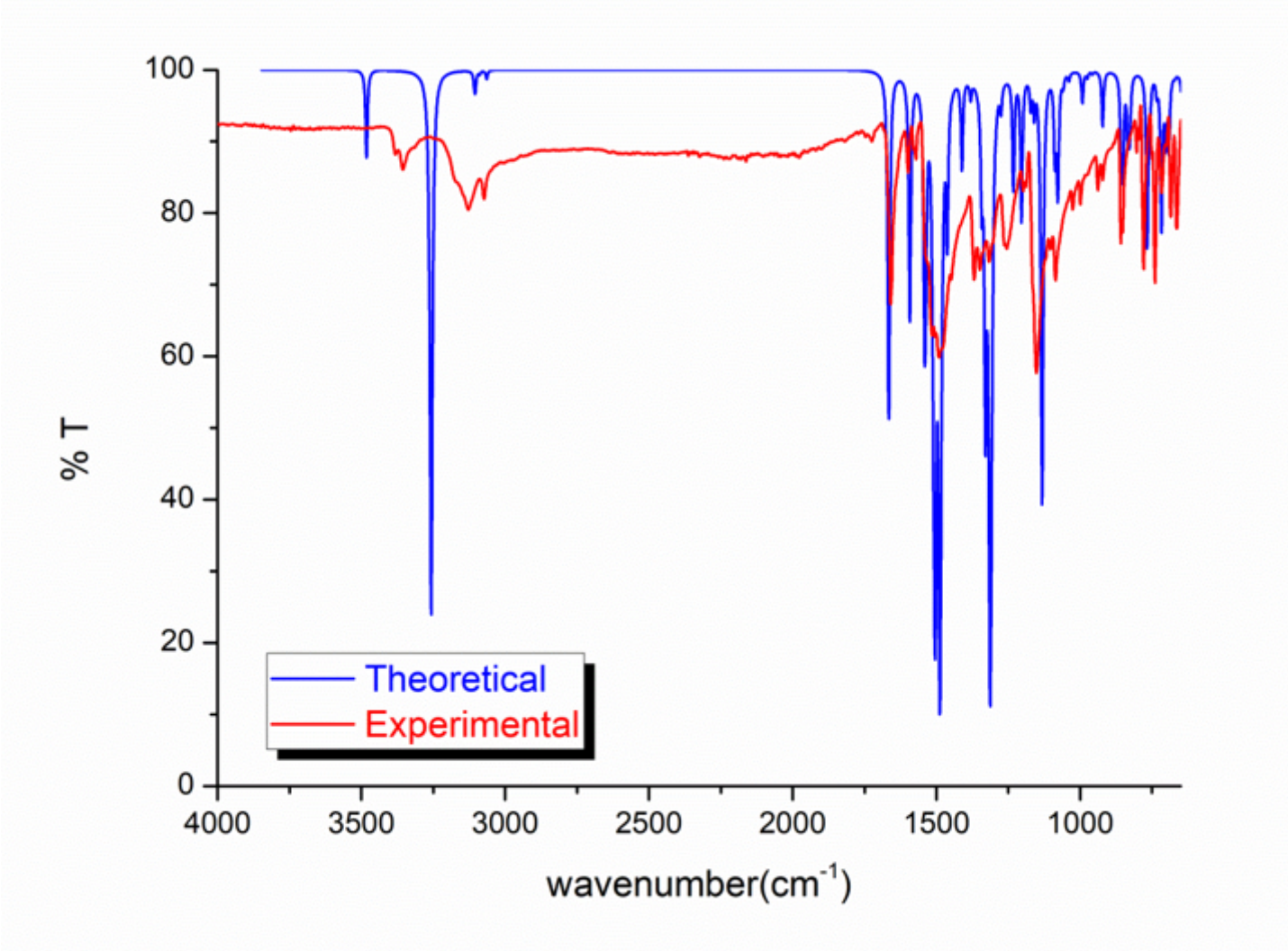

Figure 4

Experimental FT-IR and simulated FT-IR spectra of the title compound (II).

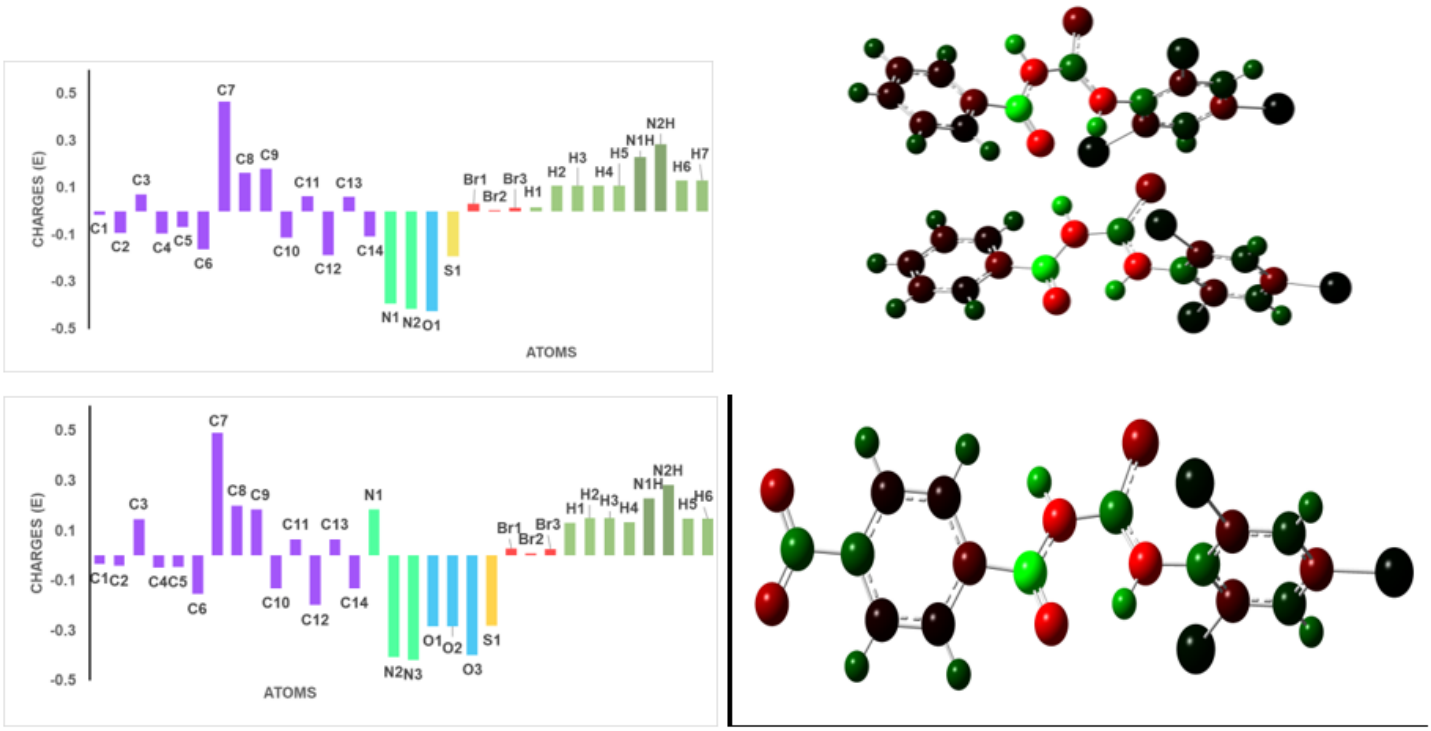

Figure 5

The Mulliken atomic charge distribution of the title compounds I and II in the gas phase.

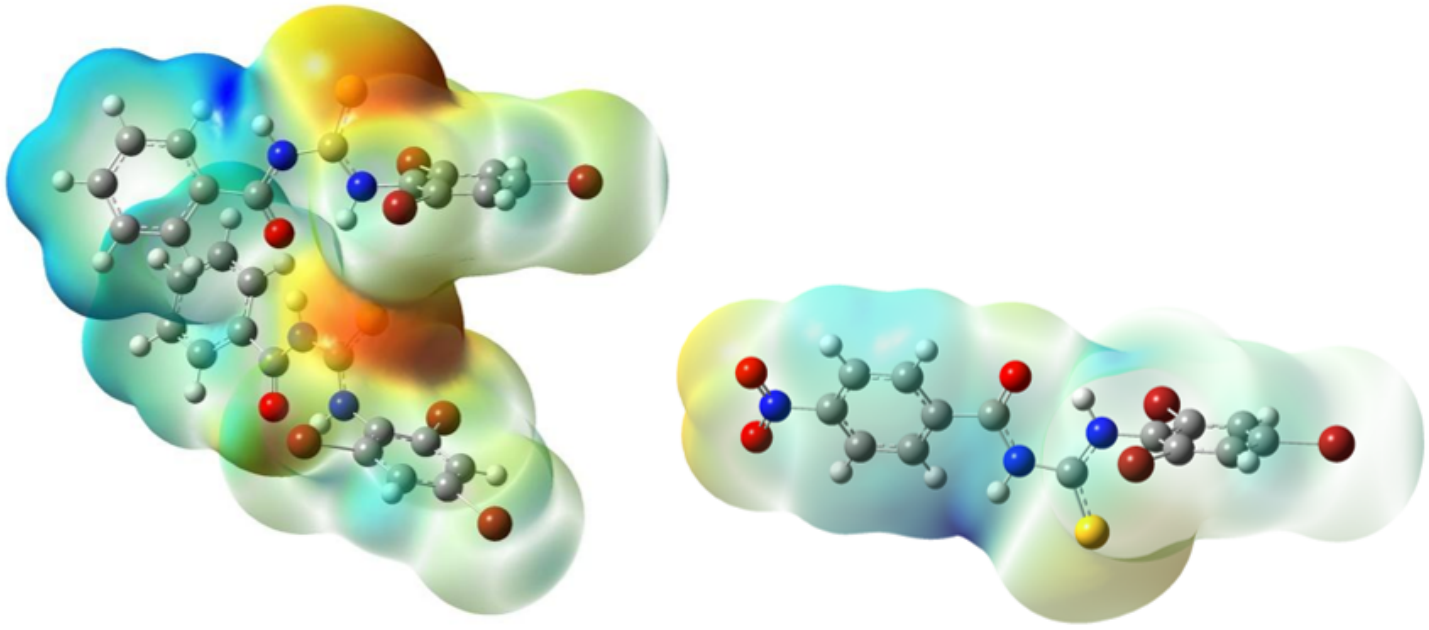

Figure 6

Molecular electrostatic potential (MEP) maps calculated at B3LYP/6–311G(d,p) level.

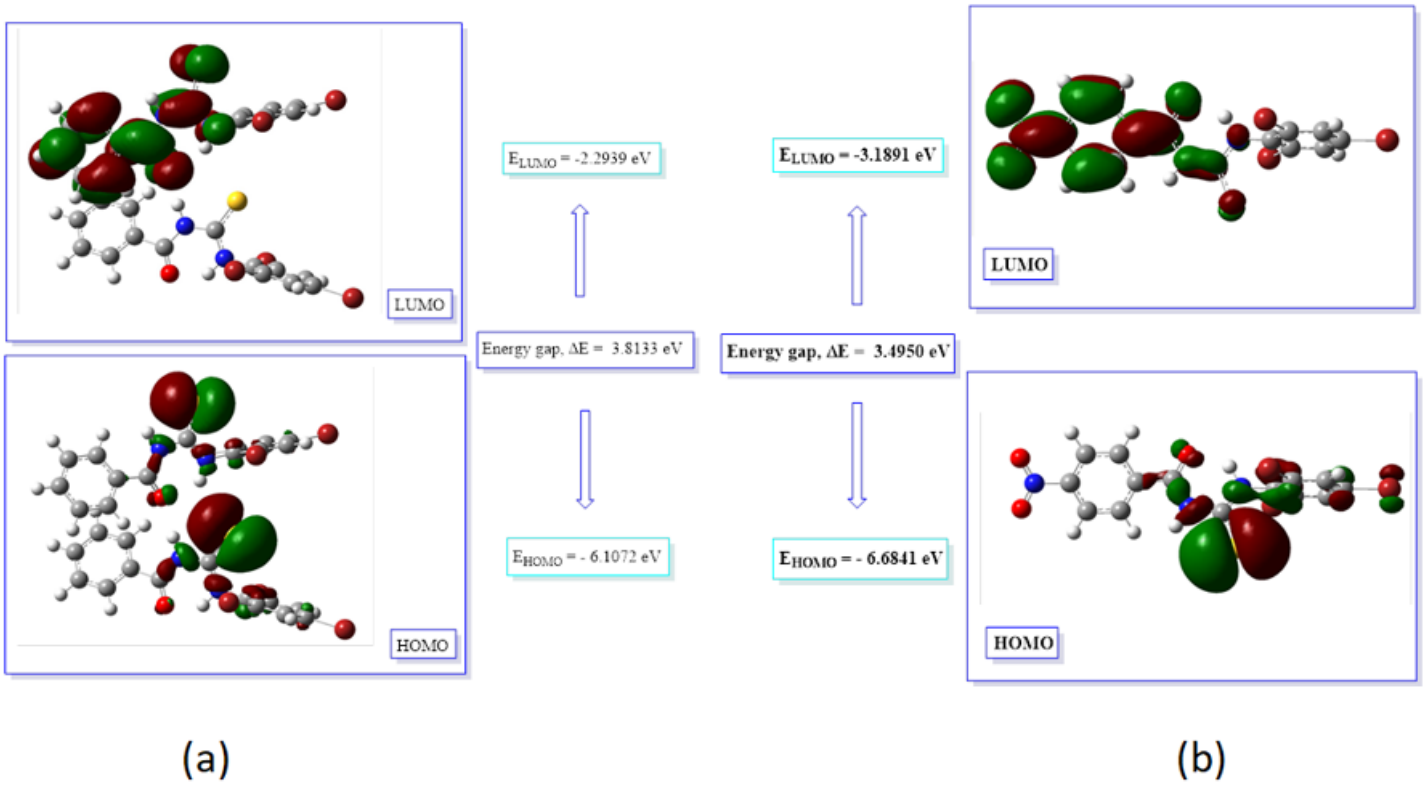

Figure 7

HOMO-LUMO plot of the title compounds (I) (a) and (II) (b).

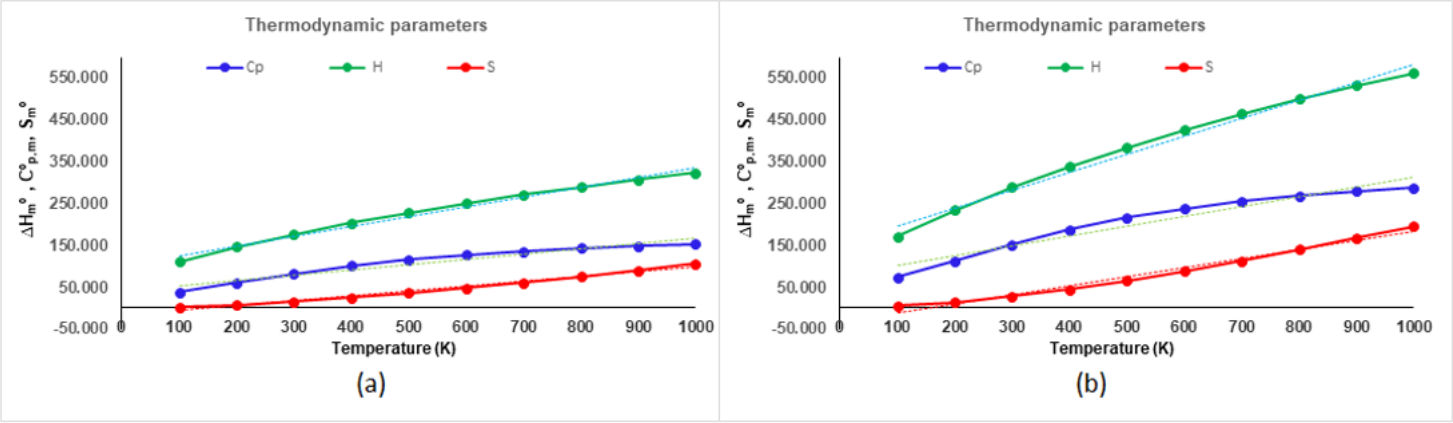

Figure 8

The thermodynamic parameters of the title compounds (I) (a) and (II) (b).

Supplementary Files

This is a list of supplementary files associated with this preprint. Click to download.

- Supplementarymaterial.docx

- Scheme1.png
- Scheme2.png